2015

Temperature Dependence Of Shear Speed In Micellar Fluid

E.G. Sunethra Kumari Dayavansha
University of Mississippi

TEMPERATURE DEPENDENCE OF SHEAR SPEED IN MICELLAR FLUID:

A Thesis
presented in partial fulfillment of requirements
for the degree of Master of Science
in the Department of Physics and Astronomy
The University of Mississippi

by

E.G. Sunethra K. Dayavansha

August 2015

ABSTRACT

Wormlike micellar (WM) fluids are viscoelastic and can support shear waves. Phase transitions of the micellar aggregates are temperature dependent and can manifest as sharp changes in the shear wave speed as a function of temperature. Thus, shear waves provide a good tool for detecting the existence of phase transitions. In this work, the variation of shear speed with temperature of 200mM CTAB/NaSal micellar fluid in a 5:3 ratio was studied. The dependence of shear wave speed on time between fluid synthesis and measurement was also investigated. Shear wave propagation through the fluid was observed as a time varying birefringence pattern by using a high speed camera and crossed polarizers and shear speed was calculated by edge tracking and wavelength measurement techniques. A gradual increase in shear wave speed was observed in the temperature range 20 - 47^{o} C. The range of shear wave speed over this temperature range is 425 - 528 mm/s. There was no any significant evidence for the time dependence of shear wave speed. Due to the absence of abrupt changes of shear wave speed, no evidence of a phase transition in this temperature range was obtained. A liquid to crystalline phase transition in the fluid was observed at lower temperatures between 6 - 7^{o} C.

ACKNOWLEDGEMENTS

I would like to express my deep sense of thanks and gratitude to my adviser, Dr. Cecille Labuda, for her encouragement and guidance throughout this research work and writing process. Her prompt inspirations, timely suggestions with kindness, enthusiasm and dynamism has enabled me to complete my thesis. I am also highly indebted and thoroughly grateful to my committee members, Dr. Joseph Gladden and Dr. Joel Mobley who rendered their valuable time and efforts for sharing their insightful comments, expertise and experience with me. I would like to thank all of the members of the Physical Ultrasonics research group for giving me all necessary assistance during this research work. I also gratefully acknowledge the staff of the Jamie L. Whitten National Center for Physical Acoustics. I am extremely thankful to my parents for supporting me spiritually throughout my life and for being a source of motivation. Finally and most importantly, I would like to thank my husband, Asela Alweera for his unconditional love, support and encouragement.

TABLE OF CONTENTS

LIST OF TABLES

LIST OF FIGURES

CHAPTER I: INTRODUCTION

INTRODUCTION

The concept of a micelle as an aggregate of surfactant molecules arose in the early part of the 19th century. In 1913, McBain was studying the anomalous concentration dependence of many physical properties of aqueous soap solutions [1]. Over recent decades, these studies of surfactant solutions has been profoundly developed by the dramatic infusion of new techniques from chemistry, physics and material science. Also, they have challenged modern physical scientists with a variety of problems involving the special nature of their structures and phase transitions. These studies are becoming more and more important because of their practical importance as detergents and as building blocks of biological membranes.

Viscoelastic wormlike micelles have attracted much interest in research because of their widespread range of applications in today's life. These fluids have been well studied and are used in the oil industry, hydraulics, and medical research. They have been successfully used in fracturing fluids in oil fields. Long, wormlike micelles are called "living polymers" because of their fascinating self-healing properties. For example, having interchangeable high and low viscoelastic properties are applicable in the processes of fracturing and transport [2]. Some of the commercial applications that have arisen from these properties, use as a drag reducing agent in heating and cooling fluids [2] [3] , increasing viscosity in personal washing products and hard surface cleaning [4] [5].

Wormlike micelles have received considerable attention from theoreticians and experimentalists due to their remarkable rheological properties. Viscoelasticity has led several researchers to use these fluids as reference systems for the testing of new experimental techniques [6]. The preparation of fluids with predefined properties is a high priority need in research. These wormlike micelles can be used to engineer many properties like mechanical and dynamic properties at the molecular level in order to design fluids with required characteristics. For example, in nanobiotechnology, bio-inspired groups are embedded into amphiphiles so that they provide the basis for safer delivery of toxic drugs [7].

Further, these wormlike micellar (WM) fluids can provide a convenient laboratory model material to investigate the behavior of shear waves in viscoelastic media. For example, WM fluids can be used to model the viscoelastic properties of tissues. It is the viscoelastic property of tissue that is important in elastography [8], a form of medical diagnostic imaging in which shear waves are used to map the elastic properties such as the Young's modulus (related to stiffness) of soft tissues in order to obtain useful diagnostic information about the presence or status of a diseased tissue like a cancerous tumor or a diseased liver. The diseased tissues have elastic properties that are markedly different from surrounding tissue. Thus, understanding the behavior of shear waves in viscoelastic media is important. For long studies, the perishability of tissue is an impediment and fixed tissue is not a good option since fixing changes the viscoelasticity of the tissue, the very property that governs shear wave propagation. A laboratory model with a non-perishable viscoelastic medium would be preferable.

In this work, we investigate the behavior of shear waves in a system consisting of a non-perishable, transparent, viscoelastic fluid known as a wormlike micellar fluid.

BACKGROUND

Wormlike micellar fluids are non-Newtonian fluids formed by the self-aggregation of surfactant molecules in an aqueous salt solution. At low concentration the surfactant molecules are dissolved as ions and the hydrophobic tails can adsorb and orient at the air-water interface, so that the surface tension (surface free energy) decreases strongly with increasing concentration (Figure 1(a)). When the concentration of surfactant reaches a particular concentration, known as the critical micelle concentration (CMC), (Figure 1(b)) the surface tension remains relatively constant because the individual surfactant molecules are saturated at the water-air surface and also in the bulk solution. If additional surfactant molecules are introduced into the fluid, the surfactant molecules spontaneously self-aggregate into micelles inside the fluid, so that the hydrophobic tails are hidden from the aqueous solution (Figure 1(c)) [9]. This hydrophobic effect minimizes the interfacial free energy of the surfactant-water system and is the main driving force for the micelle formation [10]. The, CMC is the minimum concentration of surfactant required for micelle formation. For example, the CMC of cetiltrymethylammonium bromide (CTAB, $C_{19}H_{42}BrN$), the surfactant studied in this work, is 0.92mM at 25^{o}C. To a good approximation, CMC is independent of temperature [11].

The simplest conformation of micelles is spherical. The amphiphilic surfactant molecules can spontaneously arrange in a manner that exposes their hydrophilic head groups and shields the hydrophobic tails from water molecules in aqueous solution (as shown in Figure 1(c)). A micelle is known as a dynamic structure because surfactant molecules constantly leave and enter from the micelle to the aqueous solution and vice versa [9] [10].

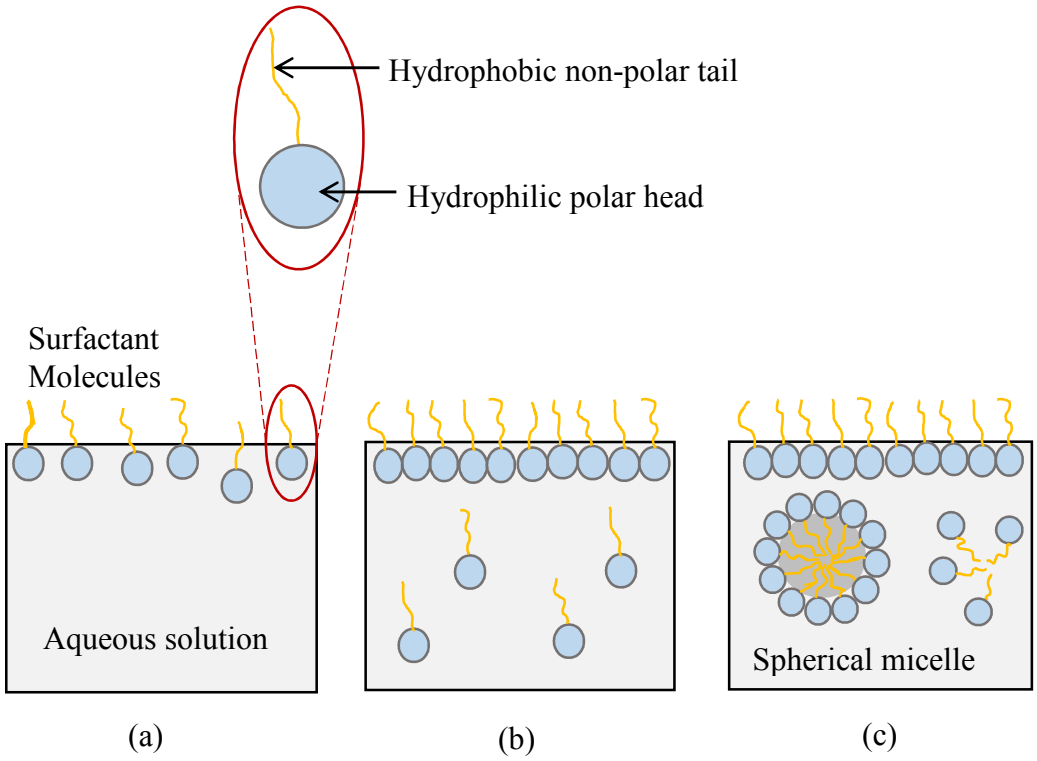

Figure 1. Diagram of surfactant molecules in aqueous solution, (a) before reaching the CMC, (b) when reaching CMC and (c) formation of spherical micelles after reaching CMC

In the thermodynamics of micellization, there are two general approaches to micelle formation. These are the phase separation model and the mass action model. In the phase separation model, micelle formation is considered as a separation of phase of micelles with unimers (individual surfactant molecules) and the CMC is the saturation concentration of surfactants in unimeric state. That is, above the CMC, the micelle concentration increases with increasing surfactant concentration, decreasing the unimer concentration. The micelle concentration can be simply approximated by the difference between total surfactant concentration and CMC. The phase separation model is appropriate for high aggregation number (the number of surfactant molecules present in a micelle) and the mass action model should be applied for low aggregation number. The mass action model describes the more gradual formation of micelles around CMC [11]. Both models describe the formation of micelles by considering the change in Gibbs free energy. Since micellization is a spontaneous process, when the CMC is below 1 M, the Gibbs free energy is negative as can be seen by considering the relation, $\Delta G = RT \ln(CMC)$ which describes the change in the Gibbs free energy of micellization at low concentrations. Although the aggregated surfactant molecules (micelles) are more ordered than the unaggregated surfactant molecules (unimers), the surrounding water molecules are highly disordered when the hydrocarbon chains of hydrophobic tails are hidden inside micelles. This significant gain of entropy of the disordered surrounding water molecules leads to an increase in the entropy of the system when micellization occurs. Because of this hydrophobic effect, the Gibbs free energy decreases.

Another factor which leads to this negative change in Gibbs free energy is the repulsion between polar head groups as they get closer during micellization. The reduced mobility of head

groups due to the restricted thermal fluctuations is responsible for the repulsion and drastic increase in entropy. Increasing the concentration of salt ions in the aqueous solution decreases the CMC of the surfactant [9]. When the concentration increases, the excess salt ions in the aqueous solution act to mitigate the electrostatic repulsion between the polar head groups, screening the effect that the charges have on one another [12]. For example, in cetiltrymethylammonium bromide (CTAB, $C_{19}H_{42}BrN$) /sodium salicylate (NaSAL, $C_7H_5NaO_3$), the WM fluid studied in this work, NaSAL is used to provide a strongly binding counter ion (SAL^-) with surfactant cations (CTA^+). The chemical structure of CTAB is shown in Figure 2.

If the concentration of the counter ion solvent (salt) is increased, the one-dimensional uniaxial growth of surfactant molecules leads to wormlike micelles. That is, the surfactant molecules are rearranged into a cylindrical tube [12]. Wormlike micellar fluids result from this wormlike topology of micelles. Figure 3 illustrates the dependence of topology of micelles on concentration (note that not all surfactants form spherical micelles). Microstructural experiments indicate that the diameter of a micelle cylinder is approximately 5-20 nm and the total length is on the order of few micrometers. The length of wormlike micelle decreases with rising temperature and increases with surfactant concentration [7].

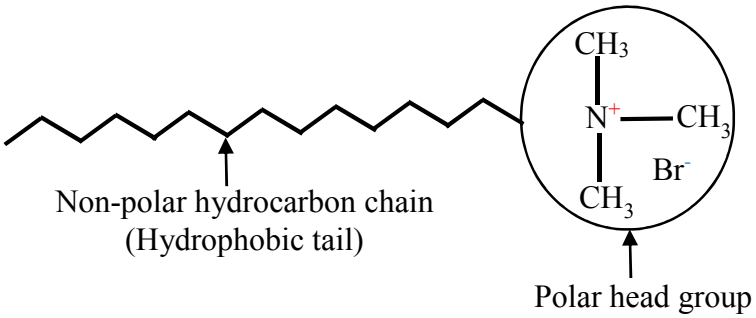

Figure 2. Chemical structure of the surfactant, CTAB

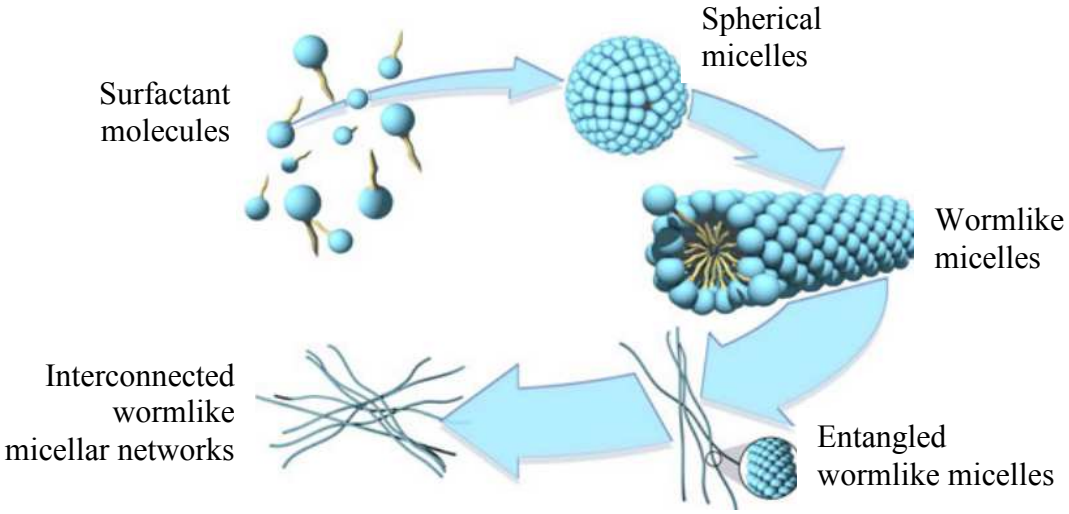

Figure 3. The variation of topology of micelles with increasing concentration
(Image: Prof. Bjorn Lindman, University of Lund, Sweden)

Micelle geometry can be characterized by the packing parameter, which, for a surfactant molecule is defined as the ratio of the volume of the hydrophobic group to the product of the length and cross sectional area of the hydrophilic group. When the packing parameter is in between 1/3 and 1/2, rodlike or wormlike micelles are expected to form [7]. It has been found that this transition from spherical micelle to wormlike micelle corresponds to a drastic increase of elasticity and viscosity of the fluid [4]. This geometry mainly depends on the type of surfactant, surfactant concentration, ionic strength of the aqueous solution, and temperature [7] [13].

For concentrations lower than the CMC, the elongation of micelles may involve large energetic barriers. However, when the concentration reaches to a well-defined saturated value, which is known as the "second CMC", the end caps of micelles are well separated by the cylindrical body minimizing the total free energy. The wormlike micellar structures are characterized by the persistence length, which is defined as the length over which the cylindrical micelle can be considered as rigid. At persistence lengths of 2 – 2.5 nm, the wormlike micelles are quite flexible and are comparable to polymers [14]. The persistence length is independent of temperature and concentration at a fixed surfactant to salt ratio. A cylindrical micelle behaves as a rigid rod when the length of the micelle is less than the persistence length and it is flexible (and wormlike) when the micellar length is greater than the persistence length [13]. From birefringence measurements, it has been estimated that the persistence length for CTAB/NaSAL micelles is 26 nm [10]. Although, little is known about the structure of the three-dimensional networks of wormlike micelles, it is known that this composition results in some important and useful fluid characteristics.

Viscoelasticity is a major consequence of this complex rheology, which is characterized by a single relaxation time according to quantitative rheological measurements [6]. The reptation relaxation mechanism [7] describes the longitudinal crossing of wormlike micelles relative to neighbors by using a random and curvilinear (snake-like) motion. This supports the occurrence of viscous flow and elastic deformation of these wormlike fluids.

The flexible and reversible structures of the fluid are responsible for the varying viscoelastic properties of the fluid. Essentially, the viscoelasticity is governed by the length of the micelle and less viscoelastic micelles display drag reduction properties. The aggregational growth of wormlike micelles by adding hydrophobic additives can boost the viscoelastic properties [2]. WM fluids also display shear-thinning (thixotropic) behavior under rapid and steady shearing. When the fluid is subjected to shear stress fields, the viscosity of the fluid decreases due to the disentanglement of the entangled network of worms. Under slow shear stresses these fluids begin flowing and tearing occurs for faster shears. These properties play a major role in generating and propagating a shear wave into the WM fluid. It has been found that these viscoelastic fluids undergo a shear banding transition, which is a transition between homogeneous to non-homogeneous states of flow, in response to steady shear [6].

The polarizability of WM fluids is anisotropic, a characteristic consequence of which is strain-birefringence. The randomly intertwined tangles of worms trapped in the fluid are optically isotropic in an equilibrium state. When isotropic entangled networks of worms are sheared, segments of the worms disengage or disentangle and partially align in the direction of the shear wave propagation [5]. This can produce domains of aligned wormlike micelles and these domains display differences in the refractive index along mutually perpendicular

directions. This phenomenon is termed strain-birefringence [16]. The relaxation through breakage and reformation of wormlike micelles can be described by the reversible scission mechanism. [7]

The index of refraction of the fluid is orientation dependent [5].Obeying the laws of normal refraction, each polarized light ray entering into the fluid is split into an ordinary ray and an extra-ordinary ray which is known as double- refraction. These emerging light rays from the micellar fluid are linearly polarized and they have polarizations mutually perpendicular to each other (as shown in Figure 4). This leads to a rotation of the polarization angle of the emerging light rays from the sheared micellar fluid. Therefore, the shearing of the fluid as the shear wave propagates through the fluid manifests as a time varying birefringence pattern. These stress fields can be visually observed by using a high speed camera, when the fluid is placed between crossed optical polarizing filters. The bright regions of the birefringence pattern correspond to shear displacement maxima and dark regions represent zero displacement [12] [17]. It is this birefringence property that is utilized to visualize and measure the speed of shear waves in the WM fluid.

The rheological properties of most viscoelastic materials are very sensitive to even small changes in temperature. Therefore, controlling the temperature of these WM fluids is required in industrial processes in order to maintain the viscoelastic properties. For example, the size of the micelle decreases monotonically with the increasing temperature [13]. Therefore viscosity decreases and water solubility increases upon heating. Although the persistence length and cross sectional radius of wormlike micelles are independent of temperature, the contour length, i.e. the length of a wormlike micelle at maximum physically possible extension, decreases

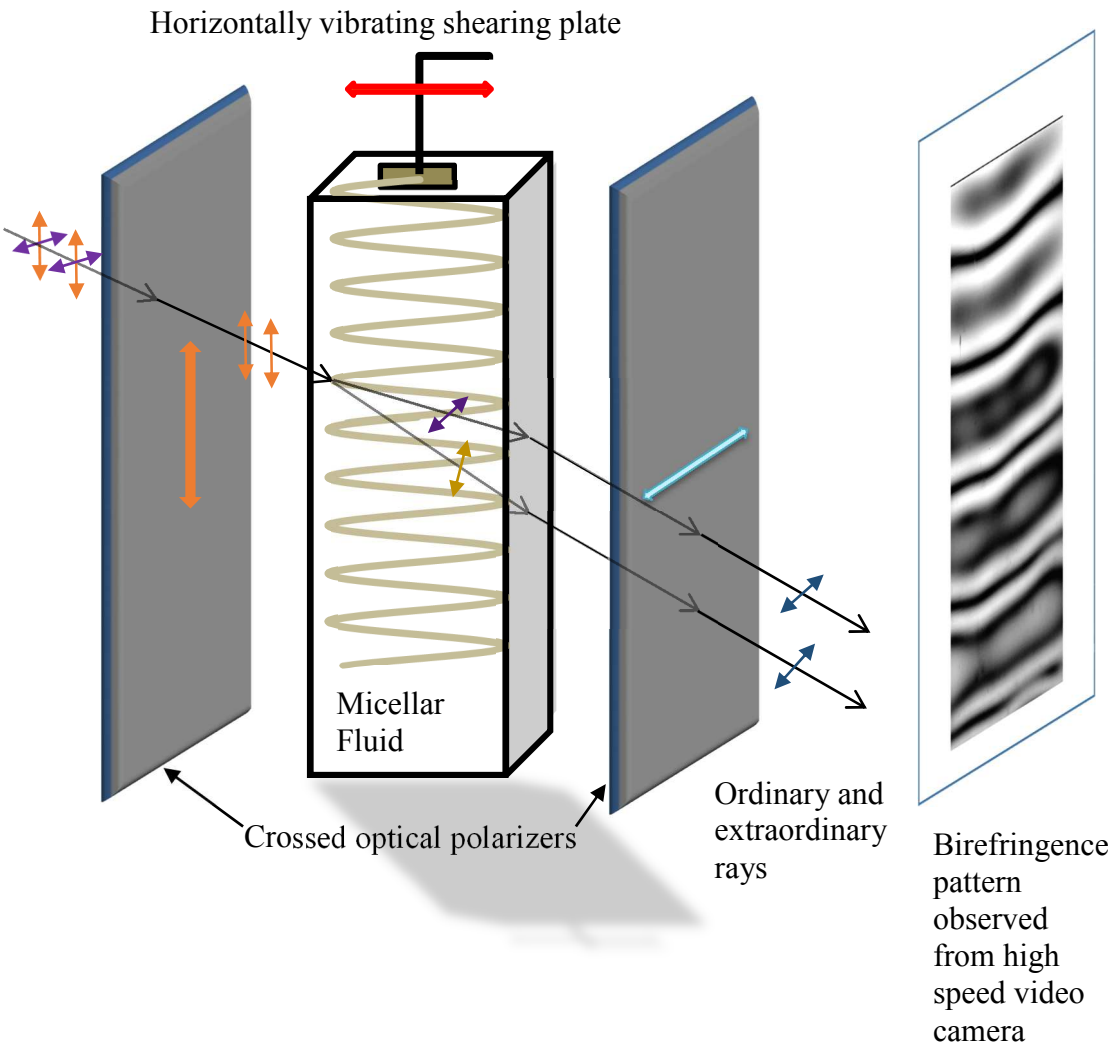

Figure 4. The formation of birefringence pattern when the shear wave is propagating through the fluid. (Un-bolded arrows indicate the path of the light rays and bolded arrows indicate polarizations)

monotonically with increasing temperature. Small Angle Neutron Scattering (SANS) observations indicates that the long wormlike micelles are formed at low temperature and they begin to break up in response to the increasing temperature. Also, they can recombine to form smaller micelles with increasing temperature [13]. Upon heating the WM fluid, the contour length of micelles decays exponentially with temperature. SANS studies show that the decrease in viscosity is associated with the decrease in micellar length. At higher temperatures, surfactant monomers in micelles start to hop between the cylindrical body and end caps rapidly. Also, it has been proposed that branching of wormlike micelles may also leads to a decrease in viscosity with increasing temperature [18].

Therefore, a general characteristic of shear thinning WM fluids is that the viscosity is decreasing with increasing temperature. Because of these temperature dependent responses of WM fluids, it is essential to study their behavior as a function of temperature. As the viscosity varies with temperature, shear stress also should vary with temperature. As a result it should affect the shear modulus and in turn the shear wave speed.

The scope of this research project was to study the variation of shear wave speed with temperature of a WM fluid in order to investigate whether these fluids undergo temperature-dependent phase transitions. The WM fluid studied here is an aqueous solution of hexadecyltrimethylammonium bromide (CTAB, $C_{19}H_{42}BrN$) and sodium salicylate (NaSAL, $C_7H_5NaO_3$) in a 5:3 ratio. This fluid can support shear waves to depths of the order of tens of centimeters depending on concentration [12] [17]. It is well known that these highly concentrated CTAB/NaSAL solutions with the surfactant/salt ratio of 5:3 form wormlike micelle structures. While SANS studies suggest that no structural transition occurs in the temperature range from 20

to 60ºC [13], measurement of shear wave speed with temperature provides an additional simple way to study phase transitions in this range. The elasticity of these fluids which originates from the microstructure of the micelles, allows the propagation of shear waves. Therefore, steep drops or changes in shear wave speed suggest phase transitions in the microstructure of the self-assembled surfactant system [12]. It has been concluded that a phase transition occurs in the 200mM CTAB/NaSAL WM fluid in concentration studies [12]. Therefore, the same WM fluid with 200mM CTAB concentration was used in these studies to investigate phase transitions by considering temperature dependence of shear wave speed.

CHAPTER II:

MATERIALS AND METHODS

EXPERIMENTAL SETUP

Micellar fluid of CTAB concentration 200 mM with a CTAB/NaSAL ratio of 5:3 was prepared by measuring out 54.67g of CTAB ($C_{19}H_{42}BrN$, Sigma-Aldrich, St. Louis MO) and 14.41g of NaSAL ($C_7H_5NaO_3$, Sigma-Aldrich, St. Louis MO). The CTAB and NaSAL were separately dissolved in 375 ml of HPLC (High Performance Liquid Chromatography) grade water (Fisher Scientific, Pittsburg, PA) to produce a 750 ml total volume of fluid. The mixtures were heated to 60^o C and mixed for about an hour on a magnetic stirrer hotplate (Fisher Scientific Pittsburgh,PA) until thoroughly dissolved. The solutions were combined and mixed for approximately 24 hours while kept warm on the stirrer plate with the beaker tightly covered with plastic wrap. The fluid was kept warm to allow air bubbles in the fluid to rise to the top. While still hot, the fluid was poured into a double-walled, cast acrylic container of 4.3 cm inner side length, 9 cm outer side length and height 30cm surrounded by a heat bath. Next, two thermocouples (OMEGA, Stamford, CT) of type E with diameter 0.51mm, were inserted into the fluid. It was allowed to sit and completely cool to room temperature for about 24 hours.

The shear wave was generated by using a 1 inch square acrylic plate mounted on a mechanical wave driver (SF-9324, Pasco Scientific, Roseville, CA). The acrylic plate was lowered until it touched the fluid surface and a 61 Hz sinusoidal signal was sent from a waveform generator (Wavetek 395, National instruments, Austin, Texas) to the wave driver to drive the plate. The plate vibrated horizontally at a frequency of 61 Hz on the fluid surface,

generating a shear wave that propagated through the fluid as a result of the horizontal vibration of the plate. Indirect visualization of the shear wave was achieved by observing the strain birefringence (see Chapter I). A backlight and diffuser were mounted to the left of the fluid and two polarizers were mounted in front and back of the fluid container with their polarization axes oriented at 90^{o} to each other. A high speed video camera (Edgertronic, FC Sanstreak Corp., San Jose, CA) with a 105mm f/2.8D lens (Nikon AF Micro Nikkor Melville, NY) was mounted to the right of the fluid to capture video of the time-varying birefringence pattern that the propagating shear wave produces. A millimeter scale was mounted in the focal plane of the lens in order to determine the pixel-to-length ratio in the focal plane. A schematic diagram of the setup is shown in Figure 5 along with a photograph in Figure 6.

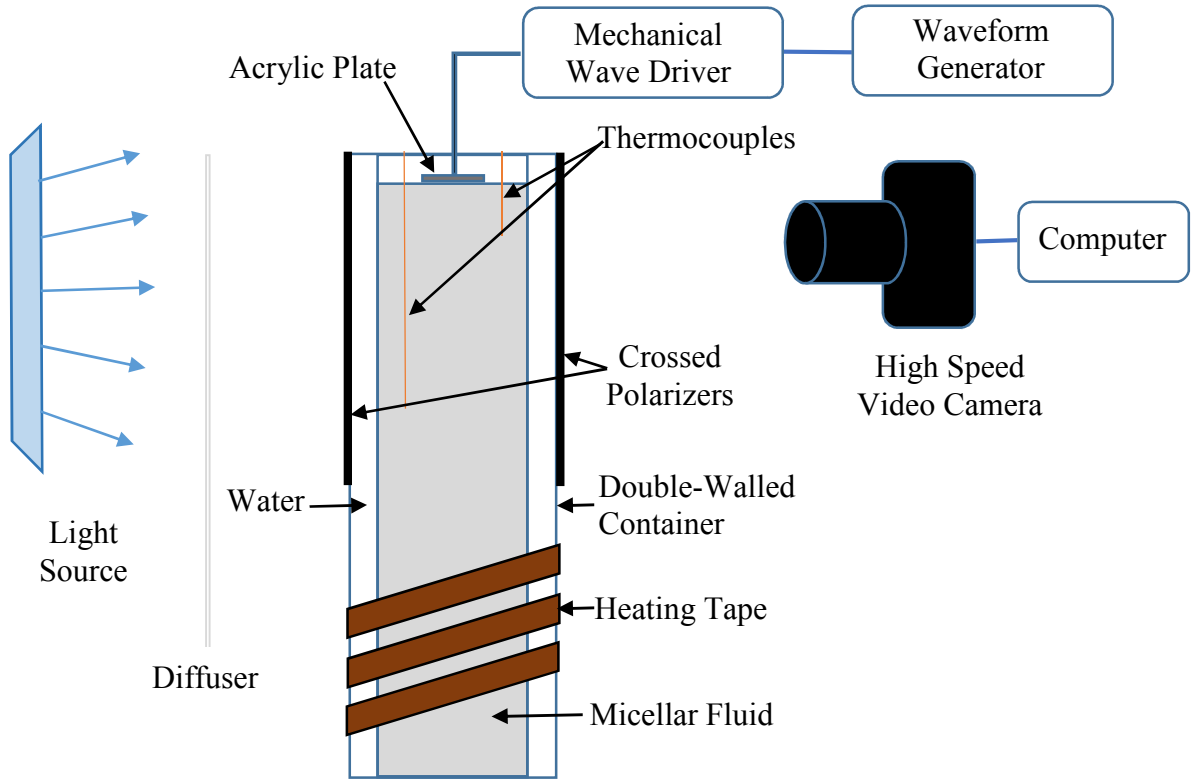

Figure 5. Schematic diagram of experimental setup

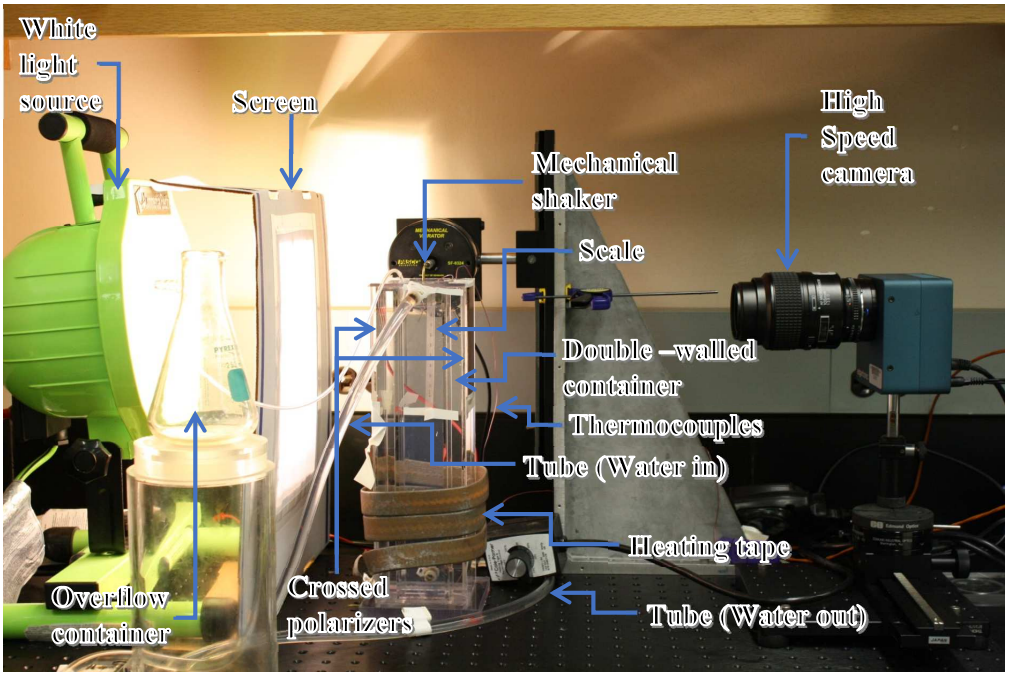

Figure 6. A photograph of experimental setup

TEMPERATURE VARIATION METHODS

Method 01 – Temperature stabilization method

The water surrounding the fluid was heated by using heating tape wrapped around the double-walled container and brought to thermal equilibrium by flowing water through a heat bath (Fisher Scientific, Isotemp 3016H, Pittsburgh, PA) which was set to a fixed temperature. The temperature readings of both thermocouples located at different positions of the fluid were recorded by allowing 15 minute time lapses for about two hours. These tempearture readings were used to observe the variation of temperature in each thermocouple with time. The fluid was considered to be in thermal equilibrium when the temperatures of both thermocouples stabilized with temperature differences between the two thermocouples of no more than 0.2^{o}C. Once the fluid was in thermal equilibrium, a high speed optical video of the propagating shear wave was obtained from the high speed video camera connected to the computer. The frame size of the video was 500 × 336 pixels and the frame rate was 2000 frames per second. This procedure was repeated for different temperatures varying from 20^{o} C to 45^{o} C in 1^{o}C increments. Also, a scale video was obtained with the millimeter scale mounted on the focal plane of the lens for pixel-to-length ratio calculations.

Method 02 – Natural cooling method

The water surrounding the fluid was heated to 50^{o}C by using the heating tape wrapped around the double-walled container and brought to thermal equilibrium by allowing water to flow from the heat bath which was set to the same temperature. The fluid was allowed to cool naturally to lower temperatures. The temperature readings of both thermocouples located at different positions of the fluid were recorded for every 1-degree drop in temperature. At each temperature, a video of the propagating shear wave was obtained and this procedure was repeated for each measured temperature until the fluid reached room temperature which was 22^{o}C. The frame size of the video was 400 × 592 pixels and the frame rate was 2000 frames per second. The height of the frame was increased from that of the previous frame, so that more than three clearly visible fringes can be used for the wavelength measurements.

CALCULATION METHODS

Pixel-to-length ratio calculation

To calculate the pixel-to-length ratio, the recorded scale video was imported into MATLAB and it was split into individual frame captures. The true color RGB images of the frames were converted into grayscale intensity images. The contrast of the images were enhanced by inverting the pixel intensity values in the intensity images and equalizing the grayscale intensity histograms (See Appendix A for the MATLAB code). As shown in Figure 7, the vertical positions of two scale markings were obtained by keeping the horizontal pixel coordinates(x) constant and recording the vertical pixel coordinates(y). The difference between these two vertical positions in millimeters was divided by the difference between the same positions in pixels to obtain the pixel-to-length ratio.

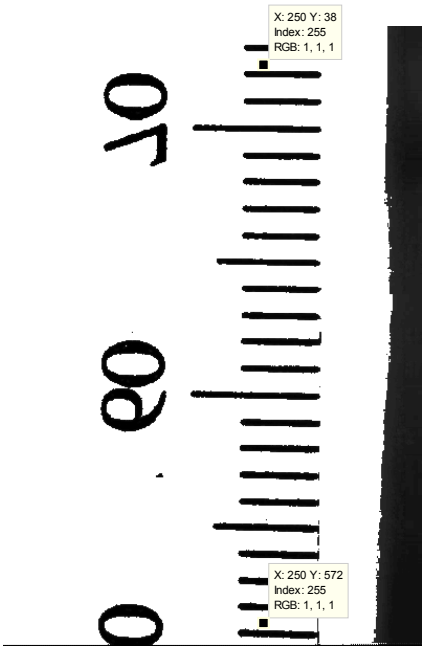

Figure 7. A frame capture of the scale video used to calculate pixel-to-length ratio

Shear wave speed calculation - method 1 (Fringe tracking method)

To calculate the shear wave speed, the recorded high speed video at a particular temperature was processed in MATLAB as described before. A set of 15 frames with an interval of 5 frames was used for the measurements. The time elapsed between these frames was 2.5 ms. This frame interval time was obtained by inverting the frame rate of 2000 frames per second and multiplying by the frame interval of 5. As shown in Figure 8, ten edges of bright fringes were selected in the first frame and manually tracked in all other frames. The horizontal pixel coordinates(x) were kept constant and the vertical pixel coordinates(y) were recorded. These vertical positions of bright fringes in each frame were used to calculate the number of pixels the shear wave propagated between frames. This calculation was repeated for 10 positions over the 15 frames and the number of pixels advanced were converted into units of length (mm) by using the pixel-to-length ratio (described in the previous section). Each of these position measurements were plotted with respect to the time elapsed as shown in Figure 9. The slopes of these 10 plots of position versus time were calculated by using the best fit line and averaged to obtain the shear wave speed in units of mm/s. The standard deviation of the 10 calculated speeds was determined. These measurements and standard deviation calculations were repeated for each temperature in the 20^{o} C to 45^{o} C range.

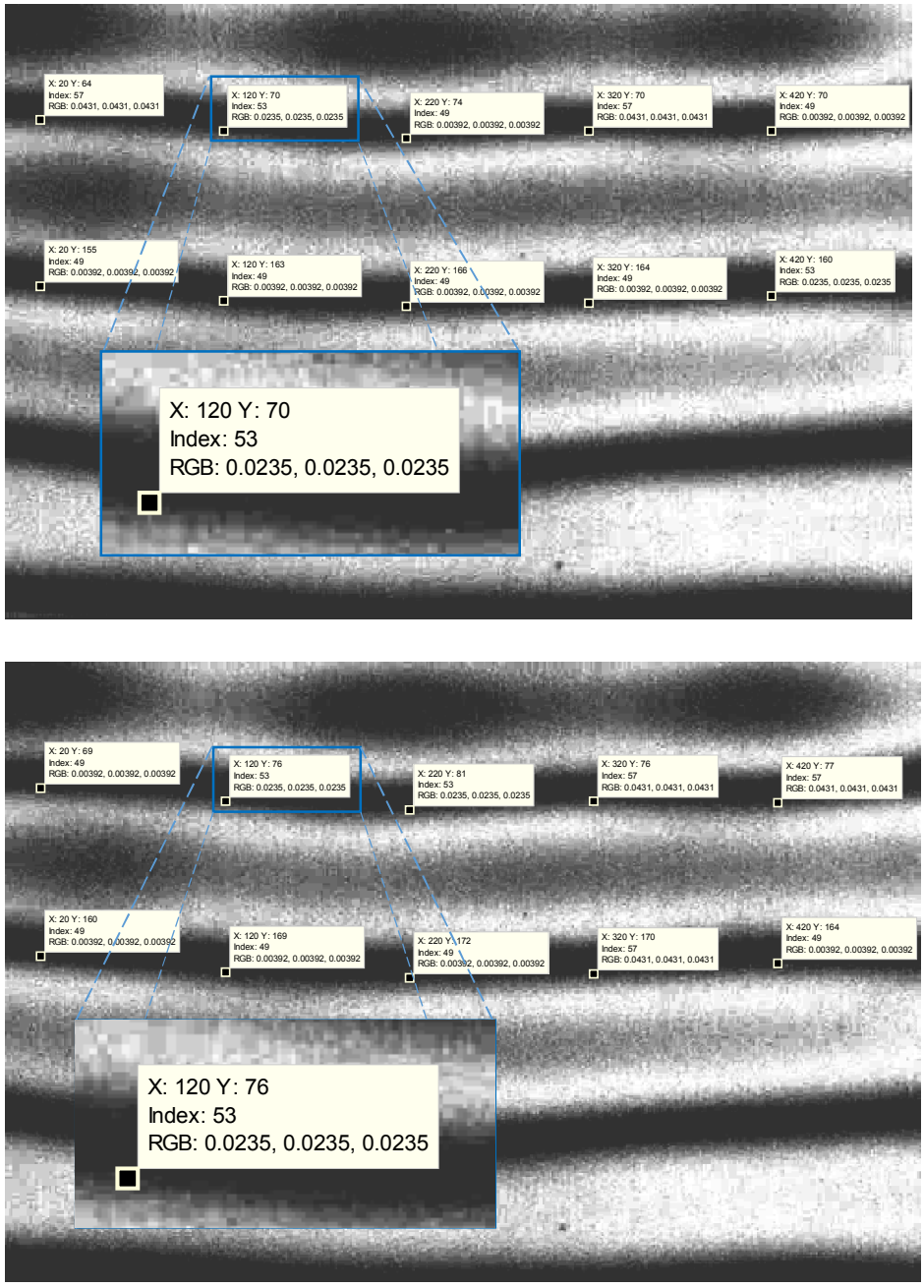

Figure 8. Two consecutive frame captures used to track 10 vertical positions of edges of bright fringes

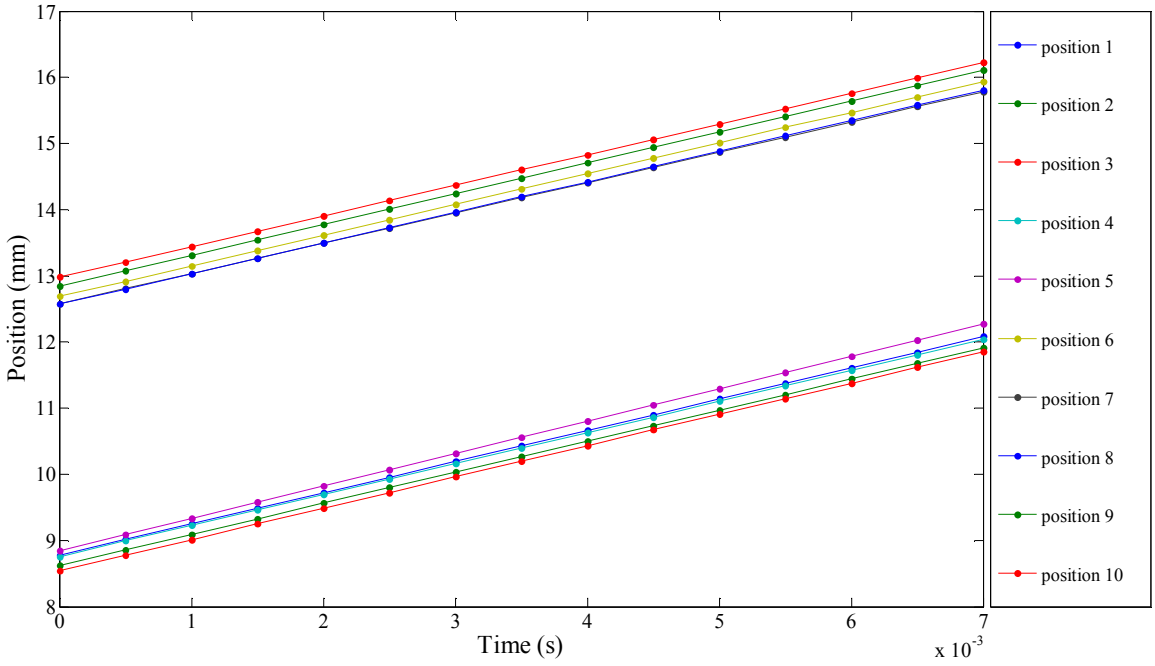

Figure 9. Plots of position versus time for 10 bright fringe edge positions over 15 frames. (Positions measured from top of frame)

Shear wave Speed calculation - method 2 (Wavelength measurement method)

The recorded high speed video at a particular temperature was imported into MATLAB and individual frame captures were obtained and converted to grayscale with contrast enhanced as before. The wavelength of the shear waves was obtained by measuring the distance from center to center of every other fringe. As shown in Figure 10, for a selected top edge position of the first bright fringe, the horizontal coordinate was kept constant and the vertical coordinates at the top and bottom of the edge were recorded. Also, for the same horizontal coordinate, the vertical coordinates at the top and bottom edges of the third bright fringe also noted. Vertical coordinates at the center of the first and third fringes were calculated by using the measured top and bottom vertical coordinates. The wavelength was obtained by calculating the difference between these vertical coordinates of the center of fringes. The obtained wavelength in pixels was converted into millimeters by using the pixel-to-length ratio. This procedure was repeated for 10 selected positions and 10 wavelength measurements were performed. The averaged wavelength, λ was used to calculate the average shear wave speed, c_s by using the relation $c_s = f\lambda$, with the pre-defined frequency, $f = 61Hz$. The standard deviation of the calculated wavelengths was obtained. These wavelength measurements and standard deviation calculations were repeated for each temperature.

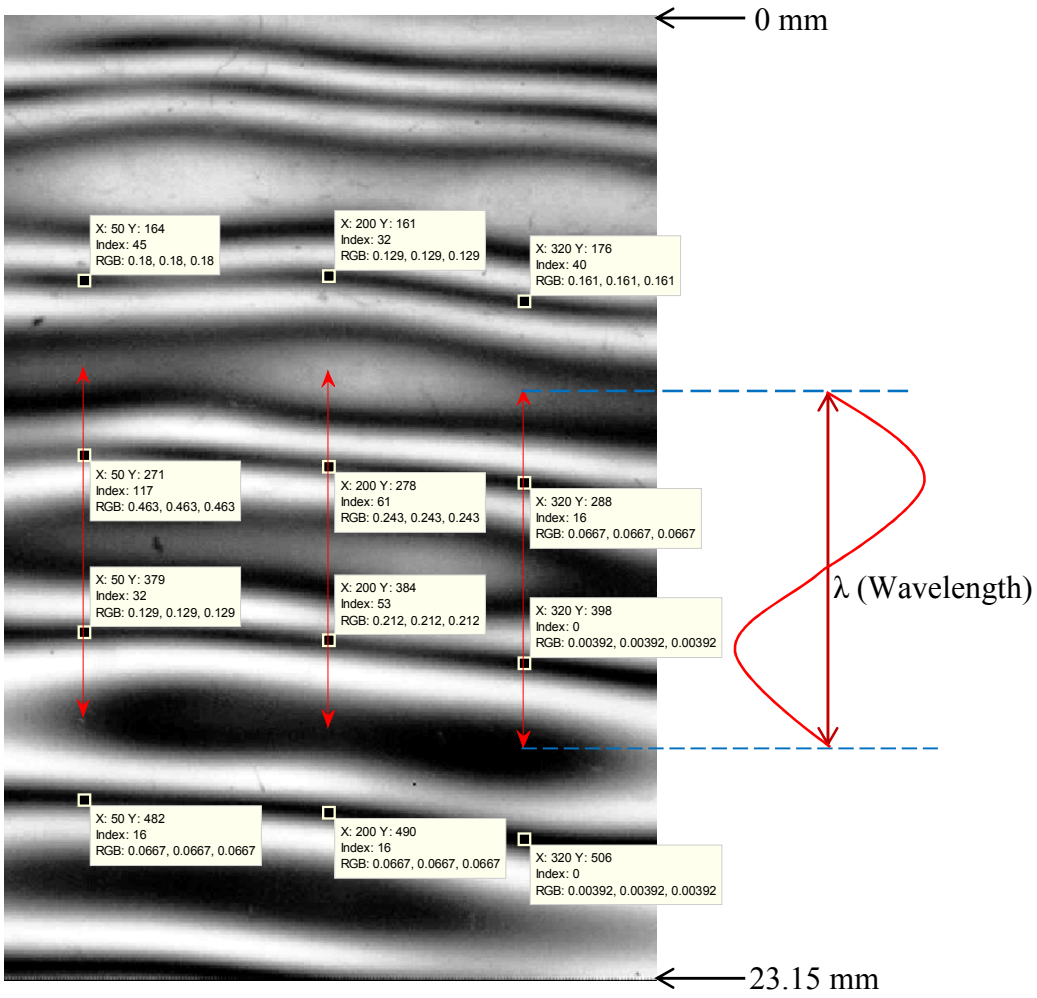

Figure 10. A frame capture used to measure the wavelength of fringes. The red double arrows indicate the wavelength measurements

CHAPTER III:

RESULTS

RESULTS OBTAINED FROM FRINGE TRACKING METHOD WITH TEMPERATURE STABILIZATION

Data set 1

Shear wave speed measurements obtained from the temperature stabilization method are summarized in Table 1. These measurements were performed soon after preparing the micellar fluid.

Figure 11, shows the measured shear wave speed data from Table 1 as a function of temperature (blue points). The average shear wave speed varies from 427-507 mm/s over the range of temperatures from 20.5^{o}C to 46.3^{o}C (range of standard deviations 6-23 mm/s). As can be seen from the figure 11, the shear wave speed increases gradually with increasing temperature. No abrupt changes in shear wave speed are seen. Also, it can be observed that the shear wave speed at large temperature greater than 42^{o}C significantly higher than that of lower temperatures. In order to confirm this result and to investigate the time dependence of shear wave speed, another data set was obtained and analyzed. (Data set 2)

Table 1. Temperature (controlled by temperature stabilization method), Shear wave speed and standard deviation in micellar fluid measured by fringe tracking measurement method

Temperature (^{0}C)	Shear wave speed (mm/s)	Standard deviation (mm/s)
20.5	452	8
23.6	427	20
24.5	425	23
25.3	441	12
26.1	429	9
26.9	437	17
27.8	435	12
28.7	443	18
29.8	432	16
30.7	428	9
31.6	429	9
32.5	426	8
33.5	418	6
34.5	430	10
35.4	439	10
36.3	443	7
37	452	17
38	428	11
38.7	442	11
39.8	452	12
40.7	456	12
41.5	452	12
41.9	474	10
42.6	492	17
43.5	497	21
44.4	473	22
45.4	494	15
46.3	507	14

Data set 2

Shear wave speed measurements were performed on CTAB/NaSAL micellar fluid with varying temperature about one month after preparing the fluid. In order to allow for a meaningful comparison of the experimental results, all the measurements were rigorously performed with the same procedure. The temperature was controlled by temperature stabilization method as before. The obtained data is summarized in Table 2.

Figure 11, shows the measured shear wave speed data from Table 2 as a function of temperature from 22.4^{o}C to 46.7^{o}C. A shear wave speed variation from 458mm/s to 514 mm/s can be observed in this temperature range without considering the error bars. Beyond 25^{o}C, the overall shear wave speed increases with increasing temperature. No abrupt change in shear wave speed was discovered, therefore there was no clear evidence of a phase transition in the studied temperature range. Also, a significant variation of shear wave speed with time could not be investigated when the range of shear wave speed of both data sets with error bars is considered. There is overlap in the error of data set in some region.

Table 2. Temperature (controlled by temperature stabilization method), Shear wave speed and standard deviation in micellar fluid measured fringe tracking measurement method (one month after preparing the fluid)

Temperature (^{0}C)	Shear wave speed (mm/s)	Standard deviation (mm/s)
22.4	483	11
23.2	469	9
24.4	464	16
25.2	458	15
26.4	461	10
27.2	464	19
28.4	476	12
29.4	465	23
30.2	461	19
31.2	473	9
32.5	473	14
33.6	486	34
34.5	488	13
35.4	482	16
36.2	501	20
37.3	488	12
38.2	486	15
39	514	18
39.9	496	15
40.8	502	14
41.9	505	15
42.9	503	8
43.9	503	12
44.9	498	9
45.7	497	7
46.7	496	10

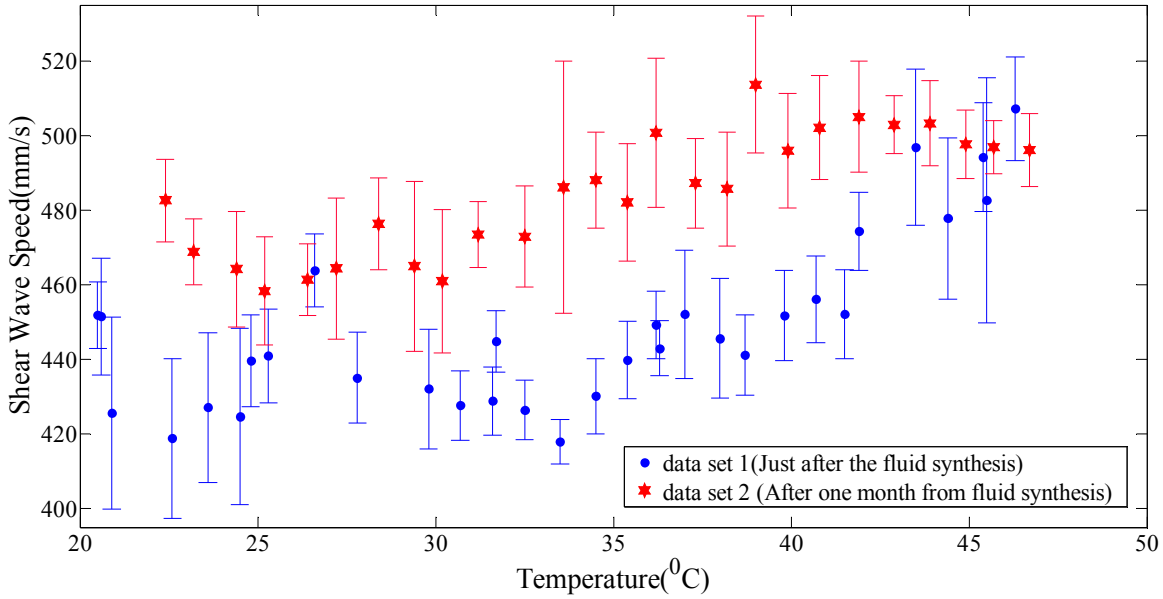

Figure 11. Plots of shear wave speed versus temperature obtained from fringe tracking method with temperature stabilization (error bars indicate twice the standard deviation)

RESULTS OBTAINED FROM WAVELENGTH MEASUREMENT METHOD WITH NATURAL COOLING METHOD

The wavelength measurements were performed from the videos obtained about six months after the preparation of the fluid. The wavelength (λ) measurements obtained from some frame captures of these videos at different temperatures are shown in Figure . These wavelength measurements indicates the shear wave propagation dependence on temperature. The shear wave speed data obtained using these wavelength measurement method is summarized in Table 3.

Figure 13, shows the measured shear wave speed data from Table 3 as a function of temperature from 22.7^{o}C to 45.6^{o}C. A shear wave speed variation from 502 mm/s to 528 mm/s can be observed in this temperature range. As with the first two data sets, a gradual increase in shear wave speed can be observed. As shown in Figure 13, any abrupt variation of shear wave speed indicating phase transition could not be observed in the studied temperature range.

Comparing with the results obtained from temperature stabilization method, the range of shear wave speed obtained from temperature stabilization method (427 - 514 mm/s) is wider than that of natural cooling method (502 - 528 mm/s) for the approximately same temperature range of 22-47^{o}C. These shear wave speed ranges indicates that the pattern of shear wave speed variation obtained from natural cooling method has been shifted from that of temperature stabilization method (as shown in Figure 14). This comparison suggests that the results obtained from the temperature stabilization method and natural cooling method are not in a very good agreement and inconclusive about any phase transition or time dependence of micellar fluid within a time period of six months in the studied temperature range.

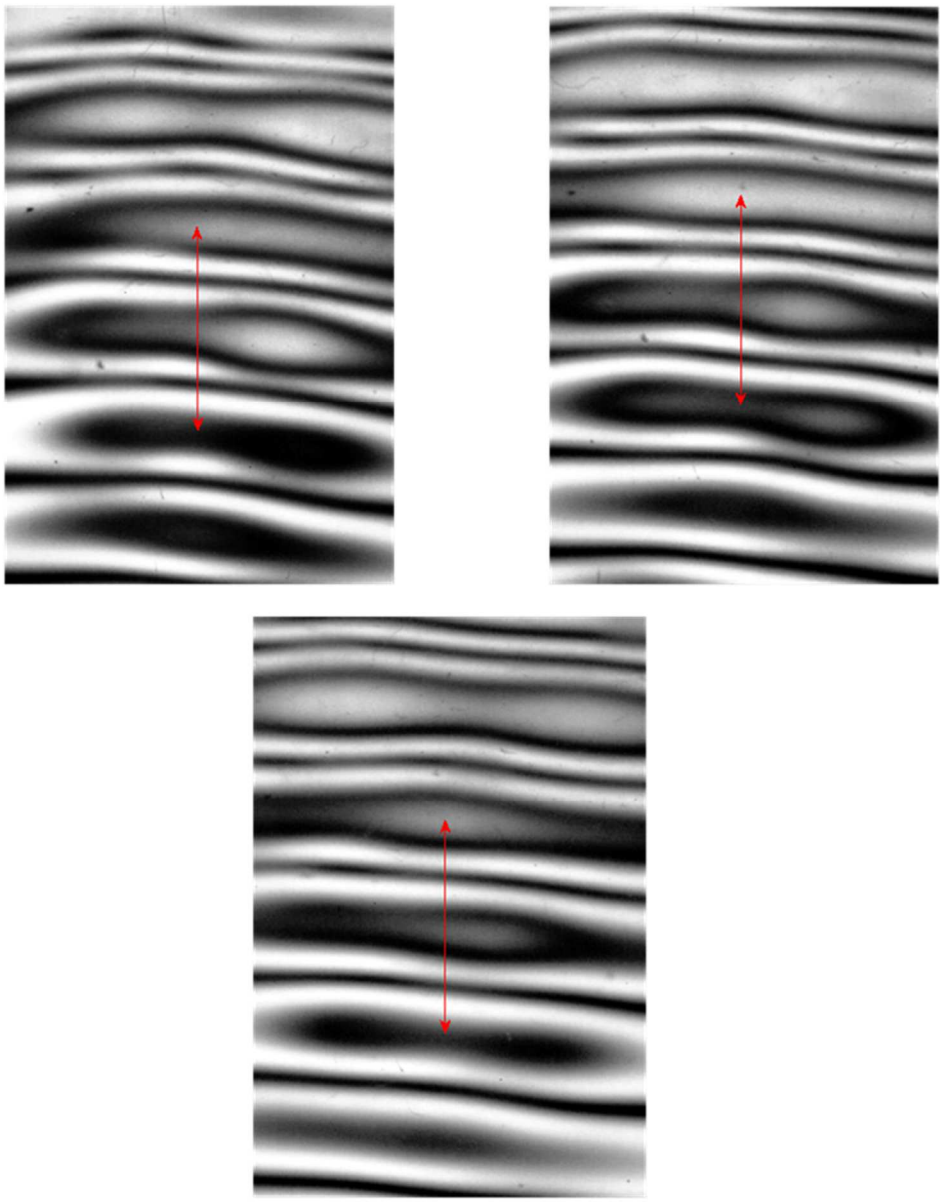

Figure 12. Wavelength measurements (indicated by red colored double arrows) obtained from a frame capture of the video at a temperature of (a) 24.3^0C (λ = 8.22 mm) (b) 34.7^0C (λ = 8.43 mm) and (c) 44.3^0C (λ = 8.65 mm)

Table 3. Temperature (controlled by natural cooling method), shear wavelength, shear wave speed and standard deviation in micellar fluid measured by wavelength measurement method

Temperature (^{0}C)	Wavelength (λ) (mm)	Shear wave speed (mm/s)	Standard deviation (mm/s)
23.7	8.36	510	6
24.3	8.22	502	6
25.3	8.27	505	7
26.2	8.44	515	6
27.2	8.35	509	7
28.1	8.40	513	6
29.0	8.33	508	8
29.9	8.37	511	6
30.9	8.46	516	7
31.4	8.35	510	6
32.7	8.48	518	8
33.8	8.40	513	6
34.7	8.43	514	7
35.8	8.42	514	5
36.7	8.61	525	7
37.8	8.42	514	6
38.8	8.41	513	7
39.8	8.56	522	7
40.9	8.58	524	7
41.9	8.43	514	5
43.1	8.63	526	8
44.3	8.65	528	8
45.6	8.46	516	5

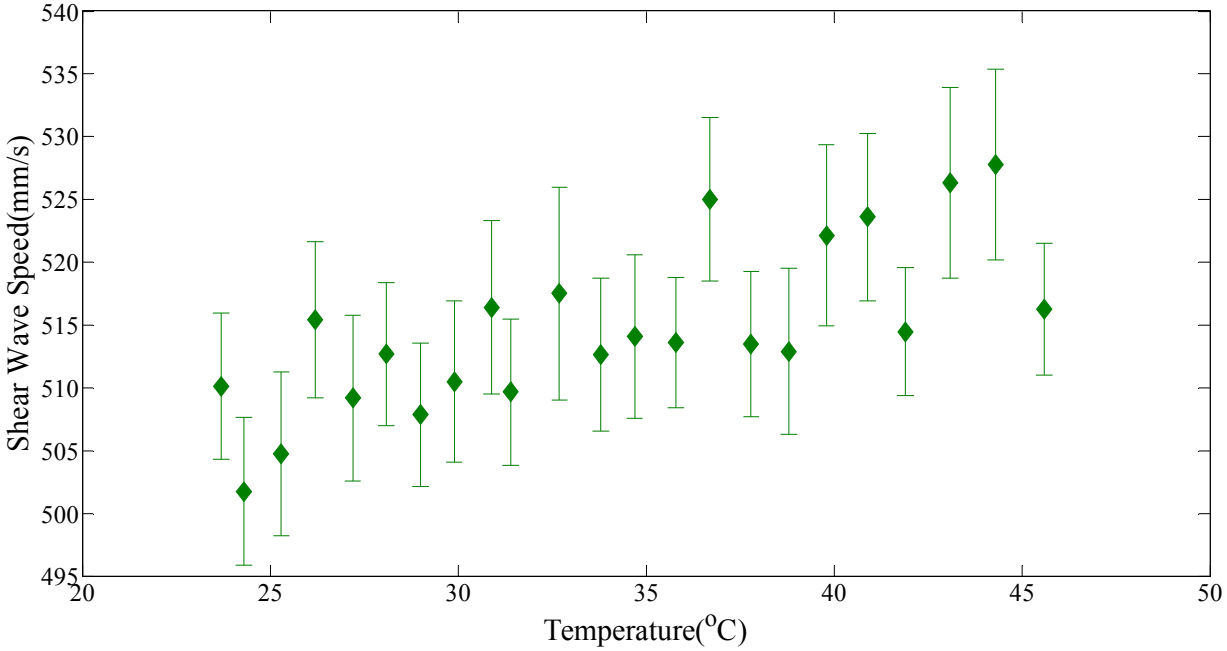

Figure 13. Plot of shear wave speed versus temperature obtained from wavelength measurement method with natural cooling (error bars indicate twice the standard deviation)

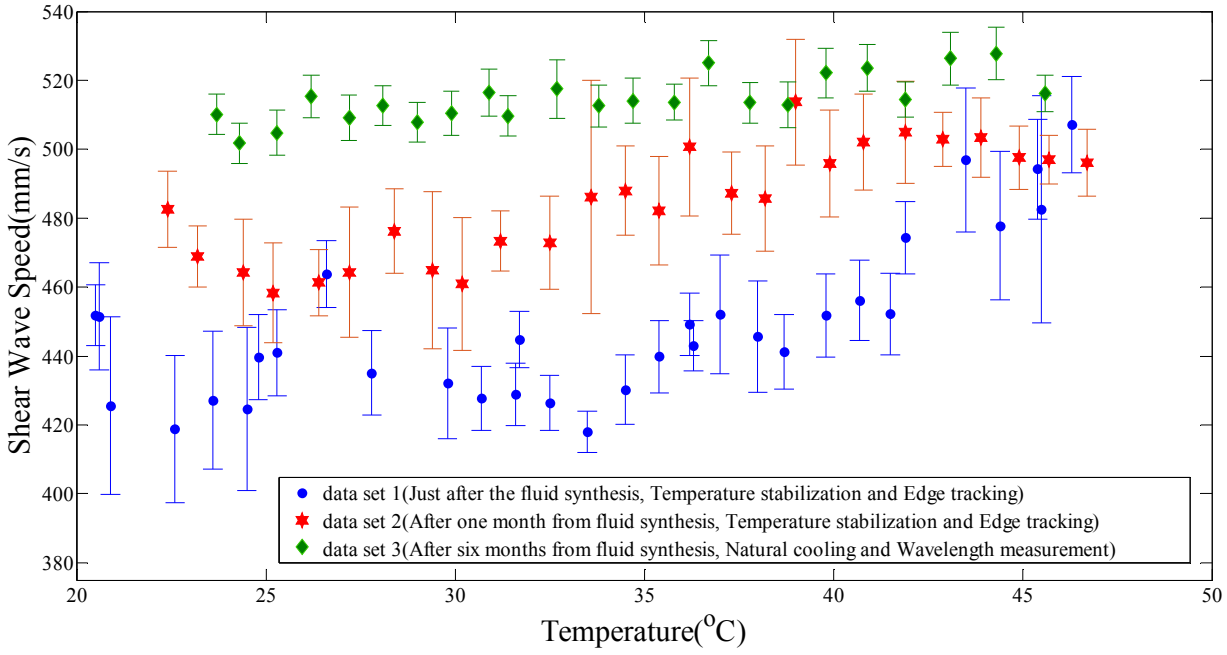

Figure 14. Plot of shear wave speed versus temperature obtained from data set 1 and 2 from edge tracking method with temperature stabilization method and data set 3 from wavelength measurement method with natural cooling (error bars indicate twice the standard deviation)

CHAPTER IV:

CONCLUSIONS AND DISCUSSION

CONCLUSIONS AND DISCUSSION

In this work, the dependence of shear wave speed on temperature in a CTAB/NaSAL micellar fluid was investigated in the temperature range 20 – 47°C. A gradual increase shear wave speed was observed in this temperature range. The average range of shear wave speed over this temperature range is 425 - 528 mm/s.

The length of the micelle is known to decrease linearly with increasing temperature [13]. This leads to decrease the viscosity of the fluid with increasing temperature. The shear wave propagation in fluids is dependent upon the viscosity and shear modulus. For highly viscous fluids like these WM fluids, it is the shear modulus that dominates the shear wave propagation [19].

In general, the shear wave speed (c_s) is controlled by shear modulus (G) and density (ρ) as shown in the following equation.

$$c_s = \sqrt{\frac{G}{\rho}}$$

Shear modulus is a quantity for measuring the stiffness by considering the deformation of the material when it experience a force. Therefore, the shear modulus is defined as the ratio of the shear stress to the shear strain.

In general, as temperature increases, the stiffness of a fluid decreases. In that case, since the shear wave speed is proportional to the square root of shear modulus, the shear wave speed

should decrease with increasing temperature, if the density is assumed to be not affected. This does not explain the obtained result of gradually increasing shear wave speed with increasing temperature in the studied temperature range. Therefore, these results suggests a gradual stiffening of the fluid with increasing temperature. It can be surmised that the behavior of shear waves in these WM fluids is complicated because of the complex structure and rheology of the wormlike micelles.

The results obtained are still inconclusive about a phase transition in the studied temperature range due to the lack of precision. Because of the relatively large standard deviations, no clear abrupt changes in shear speed are apparent. Thus, either there are no shifts in shear wave speed (indicating no phase transitions) or there are shifts hidden in the error bars. Further data analysis is required to confirm or refute the latter possibility. As shown in Figure 14, the irregular patterns and fluctuations of the shear wave speed variation with temperature suggest that further work should be done to minimize the introduction of errors. In future research, using more sophisticated methods to generate shear waves and more efficient data analysis techniques to calculate the shear wave speed would increase the precision of measurements. The errors could be minimized if an automated algorithm could be devised to track the positions of fringes instead of manual tracking. Increasing the number of tracking and measuring positions may decrease the standard deviation of shear wave speeds. This would be advantageous in the shear wave propagation studies to determine the phase transitions and aging effects of the WM fluid. Performing experiments with different techniques would provide a better understanding of the dependence of these measurements on other factors such as relaxation mechanisms and

attenuation effects. More measurements of the same series of experiments at different temperatures are necessary for better comparisons and conclusions.

Although no clear evidence of phase transitions could be observed in the temperature range of 20-47^{o}C, a phase transition from liquid state to crystalline state was observed in rough measurements around 6-7^{o}C. In future work, the range of temperature could be extended to lower temperatures in order to identify the exact temperature or temperature range at which this liquid to crystalline phase transition occurs. Also, further studies should be done to investigate the behavior of shear waves at the boundary of the liquid and crystalline state of the WM fluid. The rheology of the WM fluid around this temperature should be examined.

As shown in Figure 14, the two results obtained from the temperature stabilization method one month apart and the result obtained from wavelength measurement method six month later has been shifted from each other so that the overall shear wave speed ranges of the three data sets are increasing respectively with time. The shift of shear wave speed in these results could be due to increasing concentration of the fluid due to evaporation in the heating and cooling process. Although a plastic wrap was used to cover the top surface of the fluid in order to reduce the effect of evaporation, there can be effects of evaporation when heating the fluid several times and removing the wrap when taking data. The evaporation of water at the top surface of the micellar fluid and sticking the fluid with the shearing plate may change the concentration of the fluid when the experiments are performed several times. Maintaining the same concentration of the surfactant is vital in order to compare the results from the series of experiments.

Additionally, at some temperatures, shear wave speed measurements of all three data sets are overlapping with the contribution of error bars (Figure 14). These measurements suggest a time dependence of the acoustic properties of WM fluid. As supported by shear speed measurements over time, there can be a gradual stiffening of the fluid with time.

There are several possible sources of uncertainty in the experimental measurements. The experimental techniques should be improved to control the temperature in order to confirm that the temperature is uniformly distributed in the fluid. The variation of temperature at different positions of the fluid may introduce errors into the fringe edge tracking measurements. There is very likely a temperature gradient in the horizontal direction, but this was not quantified in these measurements. The temperature gradient could be responsible for the observation of not well aligned and slanted fringe patterns of the frames obtained at some temperatures. The wall reflections of the shear wave is also a source of uncertainty and it was minimized by limiting the width of the frame captures so that the collecting measurements are obtained from the middle of the fluid. Also, the attenuation effects should be taken into account when selecting frame size of videos. Adjusting the size of the frame so that the topmost fringes are tracked would limit introducing these attenuation effects into the measurements.

In elastography imaging techniques such as Shear Wave Elastography Imaging (SWEI) and Acoustic Radiation Force Impulse (ARFI) imaging, shear waves are typically introduced using focused ultrasound. These are emerging applications of WM fluids and in order to get more realistic and useful results with these applications, using similar laboratory techniques is an important aspect. Therefore, in future studies, a high intensity focused ultrasound (HIFU) transducer will be used to generate shear waves in the WM fluid.

BIBLIOGRAPHY

[1] William M. Gelbart, Avinoam Ben-Shaul, Didier Roux, "Micelles, Membranes, Microemulsions", and Monolayers, *Springer-Verlag*, New York, 1st edition (1994), 1-90

[2] Nor Saadah M. Yusof and Muthupandian Ashokkumar, "Ultrasound-induced formation of high and low viscoelastic nanostructures of micelles", *Soft Matter* (2013) 9, 1997-2002

[3] Shi H, Ge W, Oh H, Pattison S.M, Huggins J.T, Talmon Y, Hart D.J, Raghaven S.R, Zakin J.L, "Photoreversible micellar solution as a smart drag-reducing fluid for use in district heating/cooling systems", *Langmuir* (2013) 29(1), 102-109

[4] Jiang Yang, "Viscoelastic wormlike micelles and their applications", *Current Opinion in colloid and interface science* 7 (2002), 276-281

[5] R.G. Larson, "The Structure and Rheology of complex fluids", *Oxford University Press*: Oxford, 2nd edition (1999), 551-590

[6] Richard G. Weiss, Pierre Terech, "Molecular Gels, Materials with self-assembled fibrillar networks, *Springers*, Netherland (2006), 1-13

[7] S. Ezrahi, E.Tuval, A.Aserin, "Properties, main applications and perspectives of worm micelles", *Advances in Colloid and interface Science* (2006), vol. 128-130, 77-102

[8] L.Gao, K.J. Parker, R.M. Lerner, and S.F. Levinson, "Imaging of the elastic properties of tissue-A review", *Ultrasound Medicine and Biology*, (1996) 22, 959-977

[9] Hans-jurgen Butt, Karlheinz Graf, Michael Kappl, "Physics and Chemistry of Interfaces", *Willey VCH*, Weinheim, Germany, 2nd edition (2003), 246-258

[10] Shawn C. Owen, Dianna P.Y. Chan, Molly S. Shoichet, "Polymeric micelle stability", *Nano today* (2012) 7, 53-65

[11] Krister Holmberg, Bo Jonsson, Bengt Kronberg, Bjorn Lindman, "Surfactants and Polymers in aqueous solution", *John Willey & Sons Ltd*, Chichester, England, 2nd edition (2002), 1-52

[12] J.R Gladden, A.M. Gamble, C.E. Skelton and J. Mobley , "Shear waves in viscoelastic wormlike micellar fluids over a broad concentration range", *journal of the Acoustic Society of America*, (2012) 131(3) , 2063-2067

[13] Narayan Ch. Das, Hu Cao, Helmut Kaiser, Garfield T. Warren, Joseph R. Gladden, and Paul E. Sokol, "Shape and Size of Highly Concentrated Micelles in CTAB/NaSal Solutions by Small Angle Neutron Scattering (SANS), *Langmuir* (2012) 28 (33), 11962-11968

[14] Sylvio May and Avinoam Ben-Shaul,"Molecular Theory of the Sphere-to-Rod Transition and the Second CMC in Aqueous Micellar Solutions", *Journal of Physical Chemistry B* (2001) 105, 630-640

[15] M. Cates, S. Candau, "Statics and dynamics of worm-like surfactant micelles", *Journal of Physics: Condensed Matter* (1990) 2, 6869-6892

[16] Bradley D. Frounfelker, Gokul C. Kalur, Bani H. Cipriano, Dganit Danino, and Srinivasa R. Raghavan, "Persistence of Birefringence in Sheared Solutions of Wormlike Micelles", *Langmuir* (2009) 25, 167-172

[17] C.Labuda, C.M. Tierney, E.G. Sunethra K. Dayavansha, and J.R. Gladden, "Direct visualization of shear waves in viscoelastic fluid using microspheres", *JASA Express letters* (2015), EL 456- EL 461

[18] Raoul Zana, Eric W. Kaler, "Giant Micelles: Properties and Applications", *CRC Press*: New York, 1st edition (2007), 41-72

[19] Margaret S Greenwood, Judith Ann Bamberger "Measurement of viscosity and shear wave velocity of a liquid or slurry for on-line process control", *Ultrasonics* (2002) 39, 623-630

APPENDICES

APPENDIX A

A1. The MATLAB program used to import the high speed video, split the video into frames and to enhance the contrast of the frames

```
clear all;
close all;
filename='slomo_1401988880_36.3C.mov';
[pathstr,name,ext] = fileparts(filename);
micellar = VideoReader(filename);
fprintf('Reading video file.');
video = read(micellar,'native');

nFrames = micellar.NumberOfFrames;
vidHeight = micellar.Height;
vidWidth = micellar.Width;

mov(1:nFrames) = ...
    struct('cdata',zeros(vidHeight,vidWidth, 3,'uint8'),...
           'colormap',[]);

for k = 1 : nFrames
    mov(k).cdata = read(micellar,k);
end

for i=90:1:105
    h(i)=figure;
    [im,map] = frame2im(mov(i));
    J=rgb2gray(im);

    K=histeq(J);
    imshow(K);

    axis equal;
    axis tight;
end
```

A2. The MATLAB program used to input vertical edge positions of fringes in pixels and time differences by considering 10 positions over 15 frames in order to obtain ten position versus time graphs to average the shear wave speed at a given temperature

```
ext='.mat';
temperature=input('Temperature? ');
workspacename=[num2str(temperature) ext];

%clear all;
close all;
scalefactor=0.0388;                                                    %mm
to pix
pix=[];
pix(:,1)=[226 233 238 244 251 257 263 268 275 282 286 293 299 305 312];
pix(:,2)=[223 228 234 240 246 253 259 264 271 277 282 289 296 300 307];
pix(:,3)=[220 227 232 239 243 250 257 263 269 276 281 287 293 299 306];
pix(:,4)=[226 232 237 244 250 256 262 268 274 280 286 292 298 304 311];
pix(:,5)=[228 234 240 248 253 259 266 272 278 286 291 297 303 310 317];
pix(:,6)=[327 333 339 344 351 356 364 369 376 381 387 392 399 405 410];
pix(:,7)=[323 330 336 342 347 354 361 366 372 377 383 389 395 401 406];
pix(:,8)=[324 330 335 342 347 354 361 366 372 378 384 390 395 401 407];
pix(:,9)=[331 337 343 348 355 362 367 374 379 385 391 397 403 409 415];
pix(:,10)=[334 340 346 353 359 365 371 376 382 388 394 400 406 412 418];

distance=scalefactor*pix;
time=[0,0.5,1,1.5,2,2.5,3,3.5,4,4.5,5,5.5,6,6.5,7]*10^-3;
h=figure('Color',[1 1 1]);
box on;
% Create xlabel
xlabel('Time (s)');

% Create ylabel
ylabel('Position (mm)');

hold all;
for i=1:10
%plot(time,distance(:,i),'MarkerSize',20,'Marker','.','LineStyle','none');
%lsline;
P(:,i) = polyfit(time',distance(:,i),1);
    yfit = P(1,i)*time+P(2,i);
    plot(time,yfit,'MarkerSize',20,'Marker','.');
end
avgspeed=sum(P(1,:))/10;
SD = std(P(1,:));

save(workspacename,
'avgspeed','distance','P','pix','scalefactor','SD','time','yfit' );
```

A3 .The MATLAB program used to input top and bottom edge pixel values and scale factor in order to calculate the shear wave speed at a given temperature

```
clear all;
close all;
frequency=61;


temperature=input('Temperature? ');
%frequency=input('frequency? ');
%Pixel values at top of upper fringe
fr1a=input('Fringe 1 top pixel values: ');
%Pixel balues at bottom of upper fringe
fr1b=input('Fringe 1 bottom pixel values: ');

%Pixel values at top of lower fringe
fr2a=input('Fringe 3 top pixel values: ');
%Pixel values at bottom of lower fringe
fr2b=input('Fringe 3 bottom pixel values: ');

scalefactor=input('Scale factor? ');

%Finds pixel value of center of upper fringe
center1=fr1a+(fr1b-fr1a)/2;
%Finds pixel value of center of lower fringe
center2=fr2a+(fr2b-fr2a)/2;

%Calculates distance from center of upper fringe to center of lower fringe
wavelength=(center2-center1)*scalefactor;

%Calculates speed for each wavelength value
speed=wavelength*frequency;
[a b]=size(speed);
%Calculates average speed
avgspeed=sum(speed)/b
%Calculates standard deviation of the speeds
SD=std(speed)

ext='.mat';
workspacename=[num2str(temperature) ext];
save(workspacename);
```

A4. The MATLAB program used to plot shear wave speed as a function of temperature

```
close all;
temp=[20.5,23.6,24.5,25.3,26.1,26.9,27.8,28.7,29.8,30.7,31.6,32.5,33.5,34.5,3
5.4,36.3,37,38,38.7,39.8,40.7,41.5,41.9,42.6,43.5,44.4,45.4,46.3];
sspeed=[452,427,425,441,429.12,437.03,435.13,442.81,432.14,428,429,426,418,43
0,439,443,452,428,442,452,456,452,474,492,497,473,494,507];
err=[8,20,23,12,9,17,12,18,16,9,9,8,6,10,10,7,17,11,10.8,12,11.6,12,10.4,17,2
1,21.6,14.6,14];
errorbar(temp,sspeed,err)
% hold on
%
temp=[22.4,23.2,24.4,25.2,26.4,27.2,28.4,29.4,30.2,31.2,32.5,33.6,34.5,35.4,3
6.2,37.3,38.2,39,39.9,40.8,41.9,42.9,43.9,44.9,45.7,46.7];
%
sspeed=[482.6,468.87,464.18,458.36,461.3,464.35,476.3,464.93,460.94,473.42,47
2.96,486.16,488,482.14,500.68,487.2,485.66,513.68,495.86,502.13,505.03,502.9,
503.3,497.61,496.92,496.08];
%
err=[11.05,8.8,15.5,14.5,9.6,18.9,12.3,22.8,19.2,8.84,13.5,33.8,12.9,15.7,20.
02,11.93,15.2,18.3,15.4,13.9,14.8,7.8,11.5,9.2,7.07,9.75];
% errorbar(temp,sspeed,err)
% hold on
%
temp=[23.7,24.3,25.3,26.2,27.2,28.1,29,29.9,30.9,31.4,32.7,33.8,34.7,35.8,36.
7,37.8,38.8,39.8,40.9,41.9,43.1,44.3,45.6];
%
sspeed=[510.14,501.75,504.75,515.42,509.18,512.7,507.87,510.5,516.4,509.66,51
7.5,512.66,514.1,513.62,525,513.5,512.9,522.13,523.6,514.46,526.32,527.76,516
.26];
%
err=[5.8,5.9,6.5,6.2,6.6,5.7,5.7,6.4,6.9,5.8,8.5,6.1,6.5,5.2,6.5,5.8,6.6,7.2,
6.68,5.1,7.6,7.6,5.24];
% errorbar(temp,sspeed,err)
% % hold on
title('The plot of shear wave speed vs Temperature');
xlabel('Temperature(^0C)');
ylabel('Shear Speed(mm/s)');
%axis([20 50 495 540])
```

VITA

E.G Sunethra K. Dayavansha

PMB 1205, 115 Northgate Drive Crosby Hall • University, MS 38677 • (662) 380-1866 •

sdayavan@go.olemiss.edu

EDUCATION

B. Sc., University of Peradeniya, September 2011

TEACHING EXPERIENCE

Teaching Assistant, 2013 – 2015 May

University of Mississippi,

Engineering Physics (PHYS 221, PHYS 222) Laboratory

Research Assistant, 2013 summer and 2014 summer

University of Mississippi,

Physical Ultrasonics research group

PUBLICATIONS and PRESENTATIONS

- C. Labuda, C.M. Tierney, E.G. Sunethra K. Dayavansha, and J.R. Gladden, "Direct visualization of shear waves in viscoelastic fluid using microspheres", :JASA Express letters
- Dayavansha, E. G. S. K. (2015 June) *Temperature Dependence of Shear Wave Speed in a Wormlike Micellar fluid* presented at the Mississippi Regional Biophysical Consortium, University of Mississippi
- Dayavansha, E. G. S. K. (2015 April) *Higher Temperature Studies of Shear Wave Speed in a Wormlike Micellar fluid* poster presented at the 5th Graduate Research Forum, University of Mississippi
- Dayavansha, E. G. S. K. (2015 February) *Temperature studies of Shear Waves in Viscoelastic Micellar fluids* presented at the Rhodes College, Mississippi
- Dayavansha, E. G. S. K. (2015 January) *Temperature Dependence of Shear Wave Speed in a Viscoelastic Wormlike Micellar fluid* presented at the American Physical Society Conferences for Undergraduate Woman in Physics (APSCUWiP), University of Mississippi